IOPscience iopscience.iop.org

Home Search Collections Journals About Contact us My IOPscience

Electronic properties of $LaAlO_3/SrTiO_3$ n-type interfaces: a GGA+*U* study

This content has been downloaded from IOPscience. Please scroll down to see the full text.

2017 J. Phys.: Condens. Matter 29 095501

(http://iopscience.iop.org/0953-8984/29/9/095501)

View the table of contents for this issue, or go to the journal homepage for more

Download details:

IP Address: 137.250.129.198
This content was downloaded on 27/01/2017 at 16:38

Please note that terms and conditions apply.

IOP Publishing Journal of Physics: Condensed Matter
J. Phys.: Condens. Matter **29** (2017) 095501 (7pp) doi:10.1088/1361-648X/aa57ac

Electronic properties of $LaAlO_3/SrTiO_3$ n-type interfaces: a GGA+*U* study

I I Piyanzina[1,2], T Kopp[2], Yu V Lysogorskiy[1], D A Tayurskii[1] and V Eyert[3]

[1] Institute of Physics, Kazan Federal University, Kremlyovskaya St. 18, 420008 Kazan, Russia
[2] EP VI and Center for Electronic Correlations and Magnetism, Universität Augsburg, Universitätsstraße 1, 86135 Augsburg, Germany
[3] Materials Design SARL, 42 Avenue Verdier, 92120 Montrouge, France

E-mail: irina.piyanzina@physik.uni-augsburg.de

Received 24 November 2016, revised 22 December 2016
Accepted for publication 9 January 2017
Published 27 January 2017

Abstract

The role of electronic correlation effects for a realistic description of the electronic properties of $LaAlO_3/SrTiO_3$ heterostructures as covered by the on-site Coulomb repulsion within the GGA+*U* approach is investigated. Performing a systematic variation of the values of the Coulomb parameters applied to the Ti 3*d* and La 4*f* orbitals we put previous suggestions to include a large value for the La 4*f* states into perspective. Furthermore, our calculations provide deeper insight into the band gap landscape in the space spanned by these Coulomb parameters and the resulting complex interference effects. In addition, we identify important correlations between the local Coulomb interaction within the La 4*f* shell, the band gap, and the atomic displacements at the interface. In particular, these on-site Coulomb interactions influence buckling within the LaO interface layer, which via its strong coupling to the electrostatic potential in the LAO overlayer causes considerable shifts of the electronic states at the surface and eventually controls the band gap.

Keywords: LAO/STO heterostructure, electronic structure, GGA+U

(Some figures may appear in colour only in the online journal)

1. Introduction

The metallic heterointerface between two insulating oxides [1], namely, polar $LaAlO_3$ (LAO) and non-polar $SrTiO_3$ (STO) is continuously attracting high interest (see, for example, the recent reviews [2, 3]). The metallic conductivity occurs when the LAO overlayers reach a critical thickness and the impending polar catastrophe is mitigated by charge transfer from the LAO surface to the STO side of the interface [4, 5]. However, the number of LAO layers required to generate a metallic state is still a matter of debate [6]. While experimentally a metallic interface state was found when the LAO film reaches a critical thickness of four unit cells [5], *ab initio* calculations as based on density functional theory (DFT) led to differing results.

This is to some extent due to the use of different functionals within DFT. In particular, as well known, local and semilocal exchange-correlation functionals as provided by the local density approximation (LDA) and the generalized gradient approximation (GGA) underestimate the band gap of semiconductors and insulators and therefore cast doubt on the transition point. This shortcoming may be overcome by the GGA+*U* approach, which, allows to take into account local correlations within a selected subset of orbitals [7–9]. However, results depend on the value of the on-site Coulomb interaction *U* (and the Hund's rule coupling parameter *J*) as well as on the set of orbitals these corrections are applied to. Probably the most accurate approach currently available is provided by hybrid functionals. Indeed, while from GGA calculations band gaps of 1.6 eV for STO and 3.5 eV for LAO were obtained, which are considerably smaller than the experimental values of 3.2 eV and 5.6 eV, respectively, hybrid functional calculations led to 3.1 eV and 5.0 eV [10]. Very similar values were reported by Mitra *et al* [11]. In contrast, Nazir and

 © 2017 IOP Publishing Ltd Printed in the UK

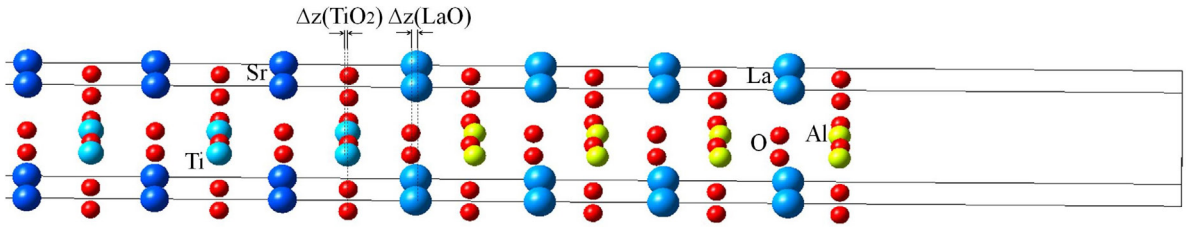

Figure 1. Heterostructure consisting of a 4LAO/4.5STO/4LAO slab (see text; only half of the structure is displayed) as arising from a structural optimization using the GGA method. Note the opposite displacements $\Delta z(TiO_2)$ of the Ti^{4+} ions and $\Delta z(LaO)$ of the La^{3+} ions relative to the O^{2-} ions of the respective same layer.

Yang opted for the GGA+U approach with $U_{La} = 7.5$ eV and $U_{Ti} = 5.8$ eV [12]. Applying these values to the parent compounds they found band gaps of 2.5 eV for STO and 3.1 eV for LAO, which are close to the GGA results.

Using the same values of U_{La} and U_{Ti} in their calculations for a heterostructure, Nazir and Yang obtained a band gap of 0.15 eV for a slab with four LAO layers and metallic behaviour beyond. This finding is in qualitative agreement with the results of Cossu *et al*, who used a symmetric slab with $5\frac{1}{2}$ central STO layers sandwiched by a varying number of LAO layers with the slabs separated by a 20 Å thick vacuum region [13]. Applying a hybrid functional they obtained a band gap of 0.6 eV for four LAO layers, while the structure with five layers was found to be metallic. However, hybrid functional calculations are computationally very demanding, which is a limiting factor especially for the study of transition-metal oxide heterostructures with large unit cells. In view of the general agreement that in these systems the electronic correlations beyond the semilocal approximation are well captured by on-site Coulomb interactions, the GGA+U approach offers a viable alternative. In adopting this approach, Breitschaft *et al* used values $U = 2$ eV and $J = 0.8$ eV at the Ti sites. In addition, in order to avoid a spurious mixing of the La 4*f* states with the Ti 3*d* bands, a large U of 8 eV was imposed on the La 4*f* orbitals [14, 15]. The necessity of introducing on-site correlations in the form of an additional Hubbard U also for the La 4*f* states to reduce their impact on the lower conduction bands was previously pointed out by Okamoto *et al*, who used yet increased values of $U_{La} = 11$ eV and $U_{Ti} = 5$ eV as well as $J_{La} = 0.68$ eV and $J_{Ti} = 0.64$ eV [16]. The same values were also adopted by Zhong and Kelly [17]. Pentcheva and Pickett used still another parameter set of $U_{La} = 7.5$ eV and $U_{Ti} = 8$ eV as well as $J_{Ti} = 1$ eV [18]. Nevertheless, an exhausting investigation of the dependence of the electronic properties on the values of U is still missing. To this end, the aim of the present contribution is to provide a systematic study of the impact of the strength of the on-site Coulomb interaction within the GGA+U approach on the electronic structure and especially the band gap of the LAO/STO heterostructures using a variety of different parameters sets.

2. Method

The *ab initio* calculations discussed in the present work were based on density functional theory (DFT) [19, 20]. Exchange and correlation effects were accounted for by the generalized gradient approximation (GGA) as parametrised by Perdew, Burke, and Ernzerhof (PBE) [21]. The Kohn–Sham equations were solved with projector-augmented-wave (PAW) potentials and wave functions [22] as implemented in the Vienna *Ab-Initio* Simulation Package (VASP) [23, 24], which is part of the MedeA® software of Materials Design [25]. Specifically, we used a plane-wave cutoff of 400 eV. The force tolerance was 0.05 eV $Å^{-1}$ and the energy tolerance for the self-consistency loop was 10^{-5} eV. The Brillouin zone of the heterostructure was sampled on Monkhorst–Pack grids of $5 \times 5 \times 1$ and $9 \times 9 \times 1$ **k**-points in order to explore the influence of the density of this mesh; for bulk $LaAlO_3$ and $SrTiO_3$ a grid of $9 \times 9 \times 9$ **k**-points was used. The GGA+U calculations were performed within the simplified approach proposed by Dudarev *et al* [26], which takes only the difference of $U - J$ into account. In the present context, we focus on the impact of the $U - J$—term as applied to the La 4*f* and the Ti 3*d* orbitals on the electronic properties. In doing so, we performed a series of spin-degenerate calculations with values for U ranging from zero to 5 eV and 9 eV, respectively, for the Ti 3*d* and La 4*f* states. For the sake of conciseness, we will use the symbol $\bar{U}$ short for $U - J$ in the text below.

The heterostructure was modeled by a central region of $SrTiO_3$ comprising $4\frac{1}{2}$ unit cells with TiO_2 termination on both sides and four $LaAlO_3$ overlayers with LaO termination towards the central slab and AlO_2 surface termination also on both sides (see figure 4 of [27] and figure 1). This slab model guaranteed a non-polar structure without any artificial dipoles. In order to avoid interaction of the surfaces and slabs with their periodic images a 20 Å vacuum region was added in accordance with previous work [13, 27]. The in-plane lattice parameter $a = b = 3.905$ Å was fixed to the experimental values of bulk $SrTiO_3$ [1] and kept fixed for all subsequent calculations reflecting the stability of the substrate. However, the atomic positions were fully relaxed. The structural relaxations caused particularly displacements of the metal atoms in the layers close to the interface relative to the oxygen atoms of the respective layers. Interestingly, these displacements point to opposite directions. To be specific, a negative displacement $\Delta z(TiO_2)$ of the Ti^{4+} ions and a positive displacement $\Delta z(LaO)$ of the La^{3+} ions relative to the O^{2-} ions of the respective same layer as indicated in figure 1 were obtained. Negative and positive here refer to displacements towards and away from the center of the full slab, which, in figure 1, is located at the left boarder of the plot.

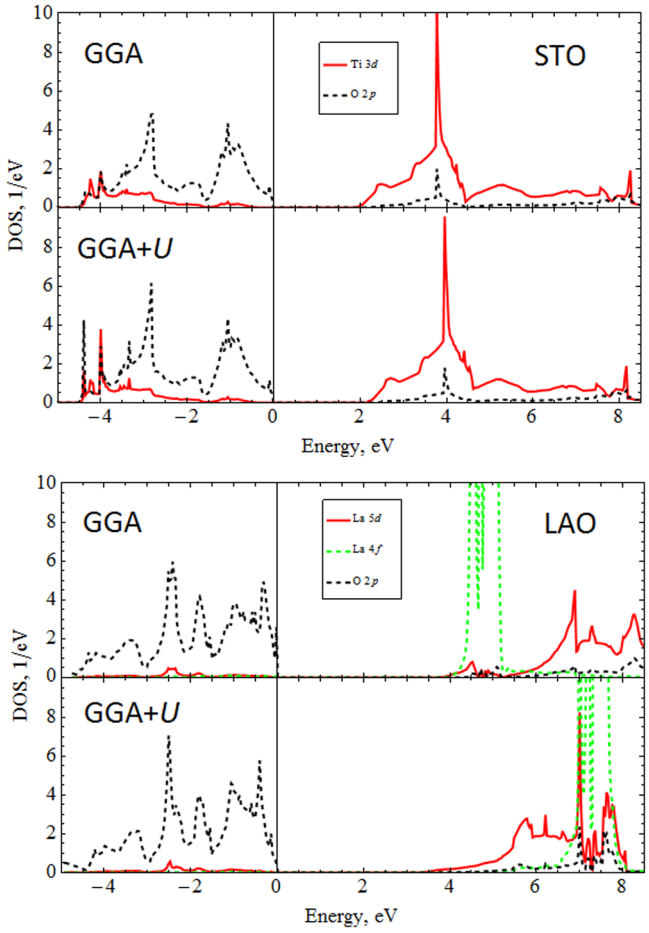

Figure 2. Densities of states (DOS) of bulk $SrTiO_3$ (top) and bulk $LaAlO_3$ (bottom) as calculated using the GGA (top) and the GGA+U method (bottom). $\bar{U}$ values of 2 eV and 8 eV were used for the Ti 3d and La 4f states, respectively.

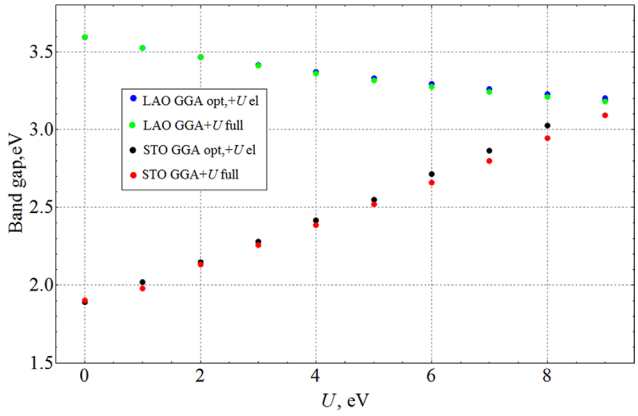

Figure 3. Calculated band gaps of $SrTiO_3$ and $LaAlO_3$ as a function of the parameter $\bar{U}$. Curves labeled 'GGA opt, +U el' refer to calculations with the structural relaxation performed at the GGA level and the GGA+U calculations used only for the calculation of the electronic properties. In contrast, curves labeled 'GGA+U full' refer to calculations, which used the GGA+U method in both steps.

3. Impact of on-site Coulomb correlations on densities of states

In a first step, we investigated the electronic properties of the constituent bulk materials, namely, bulk $LaAlO_3$ and $SrTiO_3$, and studied their sensitivity to on-site Coulomb correlations as captured by the GGA+U approach. The results are displayed in figure 2. We used $\bar{U}$ values of 2 eV and 8 eV for the Ti 3d and La 4f states, respectively. Clearly, on inclusion of on-site correlations an upshift of the Ti 3d states by about 0.25 eV and of the La 4f states by about 3 eV relative to the GGA results is observed. However, while at the same time the calculated band gap of $SrTiO_3$ is increased from 1.9 eV to 2.15 eV as expected, the band gap of $LaAlO_3$ undergoes a considerable counterintuitive decrease from 3.6 eV to 3.2 eV. According to figure 3 the dependence of the band gap of both bulk systems on $\bar{U}$ is almost linear. Obviously, the band gap depends only slightly on the level, at which the GGA+U method is applied. To be specific, we performed two kinds of calculations. In the first set, the GGA+U approach was used for both the structural relaxation and the calculation of the band gap. In contrast, in a second set of calculations the structural optimization was performed at the GGA level and the GGA+U method used only for the evaluation of the band gap. However, the effect of $\bar{U}$ on the lattice parameter, which is the only structural degree of freedom of the perovskite structure, is rather limited. To be precise, for $SrTiO_3$ the lattice parameter changes almost linearly from about 3.91 Å to 3.96 Å for $\bar{U}_{Ti}$ ranging from 0 to 9 eV and for $LaAlO_3$ it changes from about 3.78 Å to 3.80 Å within the same range of $\bar{U}_{La}$ values. These changes are similar to the differences obtained from LDA and GGA as well as their deviations from experimentally determined lattice parameters, which likewise usually do not have a large impact on the band gap.

Though the decrease of the band gap of bulk $LaAlO_3$ with increased values of $\bar{U}$ comes somewhat unexpected it can be understood from closer inspection of the partial densities of states shown in figure 2. Obviously, the La 5d states experience suppression at energies close to the La 4f states due to strong level repulsion. As a consequence, upshift of the La 4f states due to increase of $\bar{U}$ causes a suppression of the 5d density of states in the upper part of the 5d bands rather than at their lower edge. At the same time the center of gravity of the 5d bands is shifted downwards by about 1 eV. Since the lower tail of the 5d partial DOS recombines with the main part this downshift is not fully translated into a corresponding reduction of the band gap. Instead, the latter is reduced by only 0.4 eV as mentioned above. As we will see below, this mechanism is likewise effective in the heterostructure, where, however, the opposing trends of the band gaps of $SrTiO_3$ and $LaAlO_3$ in response to switching on and increasing local correlations as well as the presence of both Ti 3d and La 5d states will induce a more complex behavior.

The total and partial densities of states calculated for a slab consisting of the central STO region with four and a half unit cells sandwiched by four LAO unit cells on each side are presented in figure 4. All calculations employed a **k**-mesh of $9 \times 9 \times 1$ points. Four different points in the ($\bar{U}_{La}$, $\bar{U}_{Ti}$) parameter space are considered including GGA calculations and the set ($\bar{U}_{La} = 8$ eV, $\bar{U}_{Ti} = 2$ eV). For all sets, we observe dominant O 2p valence bands, which are (almost completely) separated

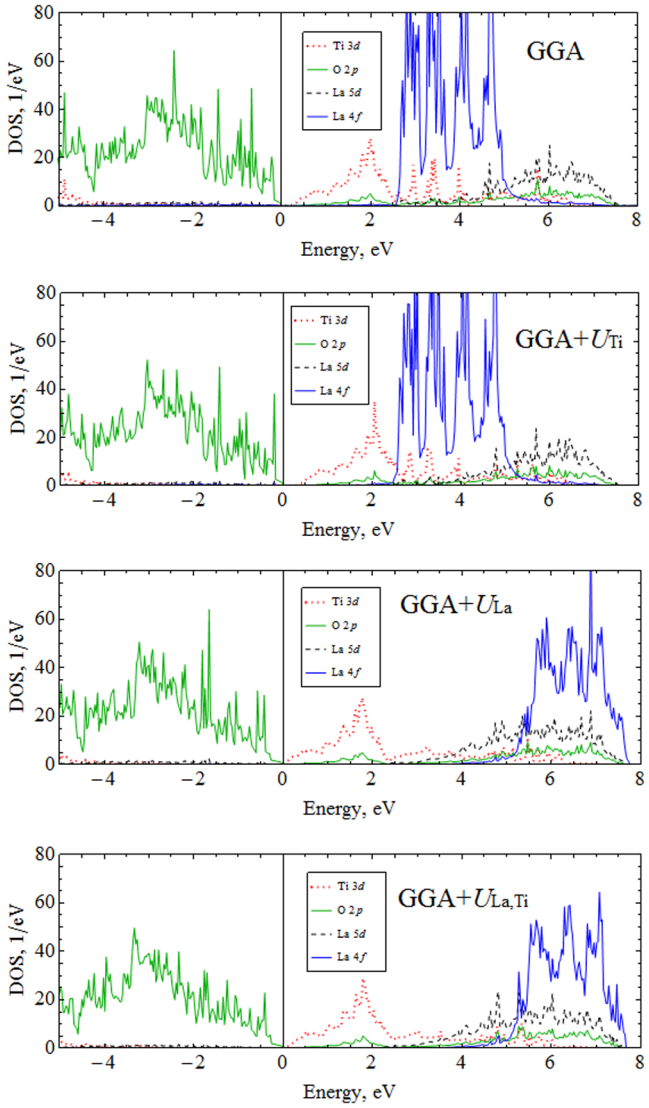

Figure 4. Densities of states (DOS) of a 4LAO/4.5STO/4LAO slab as calculated using different values of $\bar{U}$ and a **k**-mesh comprising $9 \times 9 \times 1$ points.

from the metal d and f states. Especially the latter experience considerable shifts and deformations as soon as local correlations via the $\bar{U}$ parameters are taken into account. To be specific, within the GGA semiconducting behavior with a small band gap of 0.13 eV is observed, which turns into metallic conductivity on the addition of a fifth LAO layer. This is in agreement with previous studies [12]. Worth mentioning is the overall width of the La 4f bands, which results from a distribution of single peaks of the various La atoms in the different LaO layers. As expected, on adding a $\bar{U}$ of 2 eV at the Ti sites, the band gap increases to a value of 0.25 eV while the overall shape of the partial densities of states is not affected. This changes drastically as soon as local correlations for the La 4f states are taken into account. In particular, the 4f states shift by about 3 eV just as observed for bulk $LaAlO_3$. In addition, f-wave bands originating from atoms in different planes are concentrated in a narrower energy range. Most importantly, however, a downshift of the Ti 3d bands is observed, which in turn leads to metallic band overlap for both $\bar{U}_{Ti} = 0$ eV and $\bar{U}_{Ti} = 2$ eV. While the reduction of the band gap is similar to the behavior observed for $LaAlO_3$, it is now primarily due to the Ti 3d states, which form the lower edge of the conduction band. Nevertheless, we still find considerable downshift of the center of gravity of the La 5d states with increasing $\bar{U}_{La}$. This is mainly due to the suppression of these states in the energy window between about 3 and 4.5 eV observed in the calculations with zero $\bar{U}_{La}$. In contrast, the upper part of the La 5d partial DOS between 5 and 7.5 eV is rather unaffected by the shift of the La 4f states. Restoration of the La 5d states in the range from 3 and 4.5 eV due to the upshift of the La 4f levels induced by the increased $\bar{U}_{La}$ leads to a concomitant downshift of the Ti 3d bands and, hence, to closing of the band gap. We will discuss possible origins of this behavior below.

The partial densities of states also reveal an overall similarity within the ($\bar{U}_{La}$, $\bar{U}_{Ti}$) parameter space. As even closer inspection has shown, in all cases crystal field splitting of the Ti 3d states into weakly bonding t_{2g} and well separated bonding and antibonding e_g states is found. As a consequence, the t_{2g} manifold is forming the conduction band minimum at and close to the interface. Furthermore, we observe additional splitting of these states into low lying interplanar d_{xy} states as well as d_{xz} and d_{yz} states at slightly elevated energies in agreement with previous work [28, 29]. In contrast, the latter two states become more pronounced at the conduction band minimum in TiO_2 layers away from the interface. A layer-resolved analysis of the evolution of the t_{2g} states within the central STO region of up $20\frac{1}{2}$ layer thickness has been provided in [29].

4. Layer-dependence of formation of the metallic interface

Motivated by the previous results and due to the lack of detailed studies in the literature we complemented the previous results by a systematic investigation of the dependence of the electronic properties on the values of $\bar{U}_{La}$ and $\bar{U}_{Ti}$. The results of this screening are summarized in figure 5, which displays the calculated band gaps for a variety of combinations of the two $\bar{U}$ values. The results are arranged on two sheets corresponding to the above-mentioned two different **k**-point grids with $5 \times 5 \times 1$ and $9 \times 9 \times 1$ points, respectively. Obviously, the band gap changes by about 0.1 eV on going from the coarse grid to the fine grid. However, this change is almost independent of the particular values of $\bar{U}_{La}$ and $\bar{U}_{Ti}$. Both sheets thus reflect the findings already discussed above, namely, the strong increase of the band gap with increasing $\bar{U}_{Ti}$ and its decrease with increasing $\bar{U}_{La}$.

As already discussed in connection to figure 4, interpretation of the opposing response of the band gap to the $\bar{U}$ parameters in terms of the partial densities of states and level repulsion between the d and f states is not as clear as for bulk $LaAlO_3$. We have thus inspected other calculated quantities of the heterostructure in order to identify a possible origin of the band-gap behavior, especially in dependence on $\bar{U}_{La}$. Indeed, a possible explanation is offered by the displacement of the Ti atoms out of the oxygen plane at the interface as a function of $\bar{U}_{La}$ and $\bar{U}_{Ti}$. According to figure 6 this displacement shows

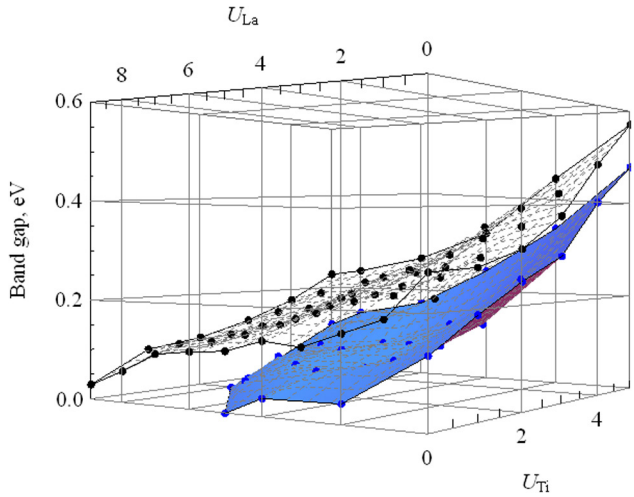

Figure 5. Calculated band gap as a function of $\bar{U}_{La}$ and $\bar{U}_{Ti}$. The black and blue points refer to calculations using **k**-point grids of $5 \times 5 \times 1$ and $9 \times 9 \times 1$ points, respectively. The dashed black and solid blue surfaces result from interpolation between the calculated band gaps and serve as guides to the eyes only.

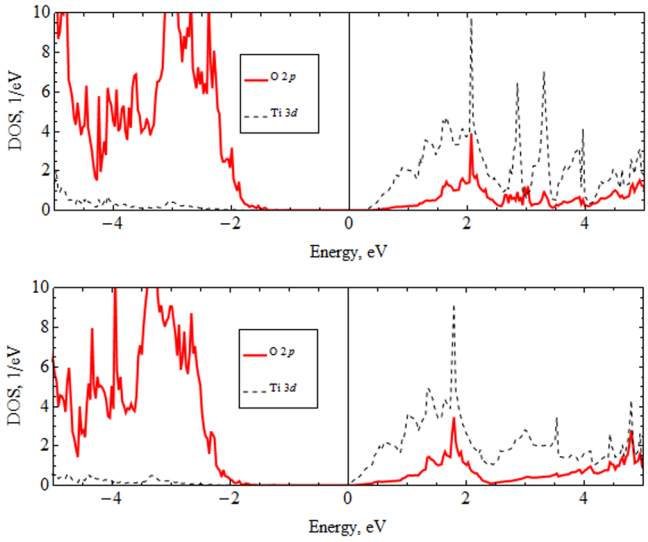

Figure 7. Partial densities of states (DOS) of a 4LAO/4.5STO/4LAO slab as calculated using the sets ($\bar{U}_{La} = 0$ eV, $\bar{U}_{Ti} = 2$ eV) and ($\bar{U}_{La} = 8$ eV, $\bar{U}_{Ti} = 2$ eV). The partial densities of states comprise contributions from atoms in the interface layer only.

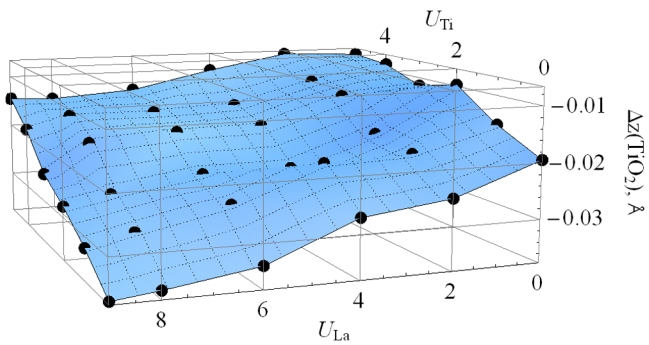

Figure 6. Displacement $\Delta z(TiO_2)$ of Ti atoms out of the TiO_2-plane next to the interface as a function of $\bar{U}_{La}$ and $\bar{U}_{Ti}$. The solid blue surface results from interpolation between the calculated points and serves as a guide to the eyes only.

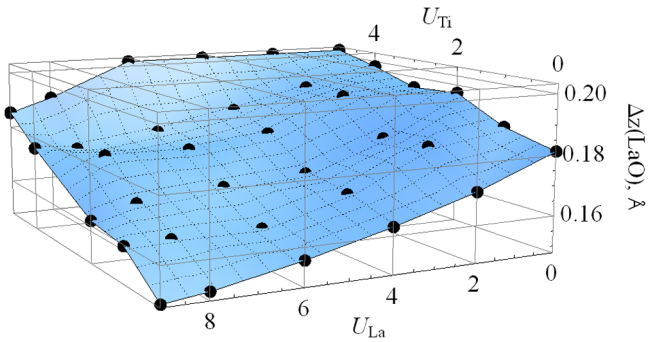

Figure 8. Displacement $\Delta z(LaO)$ of La atoms out of the LaO-plane next to the interface as a function of $\bar{U}_{La}$ and $\bar{U}_{Ti}$. The solid blue surface results from interpolation between the calculated points and serves as a guide to the eyes only.

the opposite dependence on the $\bar{U}$ values as the band gap, namely, a (negative) decrease with increasing $\bar{U}_{Ti}$ and a (negative) increase with increasing $\bar{U}_{La}$. The relation to the band gap can thus be understood in terms of a simple chemical picture based on the bonding-antibonding splitting of the Ti 3*d* and O 2*p* orbitals. A short distance between these two types of atoms as signaled by a small (negative) displacement leads to a large band gap and vice versa as is indeed observed in figure 5.

In order to check if this scenario can indeed explain the change of the band gap we calculated the partial densities of states of the atoms of the TiO_2 layer at the interface, i.e. of those atoms, which are covered by figure 6, for the sets ($\bar{U}_{La} = 0$ eV, $\bar{U}_{Ti} = 2$ eV) and ($\bar{U}_{La} = 8$ eV, $\bar{U}_{Ti} = 2$ eV). If the above scenario were valid, an increased value of $\bar{U}_{La}$ should via an increased absolute value of the displacement $\Delta z(TiO_2)$ of Ti atoms out of the TiO_2 plane induce a decreased energetical separation of the O 2*p* and Ti 3*d* bands. However, the calculated partial densities of states as displayed in figure 7 do not give any indication for such a scenario. Indeed, on going from $\bar{U}_{La} = 0$ eV to $\bar{U}_{La} = 8$ eV the O 2*p* bands are shifted downwards by the same amount as the Ti 3*d* levels. We thus have to rule out the displacement of the Ti atoms out of the TiO_2 plane at the interface as the major source of the decreasing band gap with increasing $\bar{U}_{La}$.

Next, we turn to a different scenario, which is based on the displacement $\Delta z(LaO)$ of La atoms out of the LaO plane at the interface as a function of the $\bar{U}$ parameters as displayed in figure 8. For all values of the $\bar{U}$ parameters included in the figure we find a positive displacement, which signifies that the La atoms are shifted away from the LaO interface layer, as shown in figure 1(b) of [29]. Most prominently, the shift is reduced for increasing $\bar{U}_{La}$, which according to figure 6 is accompanied by a negative displacement of the Ti atoms in the interface layer as is expected when electrostatics is accounted for. This scenario was already addressed by Zabaleta *et al* in the context of the application of hydrostatic pressure, which likewise tends to reduce the buckling in the LaO layer [29]. According to Zabaleta *et al*, the concomitant suppression of the dipole moment of this layer would reduce the screening of the polar discontinuity,

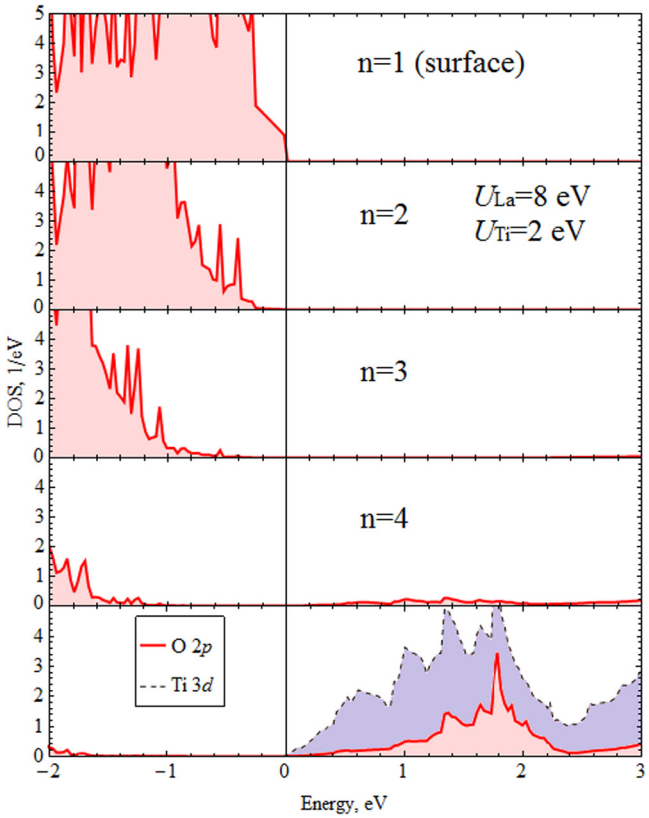

Figure 9. Partial densities of states (DOS) of a 4LAO/4.5STO/4LAO slab as calculated using the set ($\bar{U}_{La} = 8$ eV, $\bar{U}_{Ti} = 2$ eV). The partial DOS comprise contributions from atoms inside the indicated layers only (see also [15, 30, 31]).

which fact enhances the charge density at the interface [29]. In the present context we thus suggest that increasing $\bar{U}_{La}$, via the reduced dipole moment in the LaO layer and the resulting reduced screening of the polar discontinuity, eventually entails a corresponding increase of the electrostatic potential across the LAO slab. The latter induces an upshift of the surface O 2*p* states relative to the Ti 3*d* states at the interface that, according to the layer-resolved partial densities of states displayed in figure 9 (see also [15, 30, 31]), closes the band gap between these states. We thus arrive at the important conclusion that the effect especially of $\bar{U}_{La}$ on the electronic properties is only indirect since this parameter mainly controls the buckling of the LaO planes and of the TiO_2 interface plane and affects the electronic bands only via this structural characteristic.

5. Conclusions

The present study has led to a variety of important results. While for bulk $SrTiO_3$ increasing influence of local electronic correlations as captured by the on-site Coulomb repulsion parameter $\bar{U}_{Ti}$ applied to the Ti 3*d* states leads to the expected increase of the band gap, a counterintuitive decrease of the band gap with increasing value of $\bar{U}_{La}$ for the La 4*f* states of bulk $LaAlO_3$ is observed. From analysis of the partial densities of states we were able to explain this behavior by recovery of the lower conduction band of La 5*d* character from deformation due to 5*d*-4*f* level repulsion as the La 4*f* states shift to higher energies and thereby to identify the purely electronic origin of this behavior. While for the heterostructure, analysis of the partial densities of states likewise reveals increase and decrease or even closure of the band gap with increasing $\bar{U}_{La}$ and $\bar{U}_{Ti}$, respectively, as well as the 5*d*-4*f* level repulsion, a simple interpretation is spoiled by the presence of the Ti 3*d* states at the conduction band edge.

Systematic screening of the ($\bar{U}_{La}$, $\bar{U}_{Ti}$) parameter space allowed to identify correlations between different structural and electronic properties. In particular, decrease/increase of the band gap goes along with (negative) increase/decrease of the displacement of the Ti atoms out of the TiO_2 interface plane and (positive) increase/decrease of the La atoms out of the LaO interface plane. However, inspection of the partial densities of states gave no indications for a change in bonding-antibonding splitting between the O 2*p* and Ti 3*d* bands, which would explain the change in band gap in terms of the structural distortion with the TiO_2 interface layer. Following the pressure study of Zabaleta *et al* [29] we thus arrive at a non-local scenario relating the band-gap trends to the buckling of the LaO layers close to the interface, which in turn has a strong impact on the dipole moment of this layer. Reduced buckling would thus translate into reduced screening of the polar discontinuity and a stronger electric field in the LAO slab, which causes upshift of the O 2*p* valence states at the surface relative to the Ti 3*d* conduction bands at the interface and thus decrease of the band gap. In conclusion, our calculations reveal that the impact of local electronic correlations on the electronic properties is primarily due to strong electron-lattice coupling, which controls the buckling of the LaO layers close to the interface.

Acknowledgments

This study was supported by the Supercomputing Center of Lomonosov Moscow State University. The authors from KFU acknowledge partial support by the Program of Competitive Growth of Kazan Federal University. I Piyanzina received financial support from the German Academic Exchange Service (DAAD). I Piyanzina and T Kopp acknowledge support by the German Science Foundation (DFG) through TRR 80.

References

[1] Ohtomo A and Hwang H Y 2004 *Nature* **427** 423
[2] Bristowe N C, Ghosez P, Littlewood P B and Artacho E 2014 *J. Phys.: Condens. Matter* **26** 143201
[3] Gariglio S, Fête A and Triscone J-M 2015 *J. Phys.: Condens. Matter* **27** 283201
[4] Nakagawa N, Hwang H Y and Muller D A J 2006 *Nat. Mater.* **5** 204
[5] Thiel S, Hammerl G, Schmehl A, Schneider C and Mannhart J 2006 *Science* **313** 1942
[6] Chen H, Kolpak A M and Ismail-Beigi S 2010 *Adv. Mater.* **22** 2881

[7] Anisimov V I, Zaanen J and Andersen O K 1991 *Phys. Rev.* B **44** 943
[8] Anisimov V I, Solovyev I V, Korotin M A, Czyżyk M T and Sawatzky G A 1993 *Phys. Rev.* B **48** 16929
[9] Czyżyk M T and Sawatzky G A 1994 *Phys. Rev.* B **49** 14211
[10] Eyert V 2010 private communication
[11] Mitra C, Lin C, Robertson J and Demkov A A 2012 *Phys. Rev.* B **86** 155105
[12] Nazir S and Yang K 2014 *ACS Appl. Mater. Interfaces* **6** 22351
[13] Cossu F, Schwingenschlögl U and Eyert V 2013 *Phys. Rev.* B **88** 045119
[14] Breitschaft M *et al* 2010 *Phys. Rev.* B **81** 153414
[15] Pavlenko N and Kopp T 2011 *Surf. Sci.* **605** 1114
[16] Okamoto S, Millis A J and Spaldin N A 2006 *Phys. Rev. Lett.* **97** 056802
[17] Zhong Z and Kelly P J 2008 *Europhys. Lett.* **84** 27001
[18] Pentcheva R and Pickett W E 2008 *Phys. Rev.* B **78** 205106
[19] Hohenberg P and Kohn W 1964 *Phys. Rev.* **136** B864
[20] Kohn W and Sham L J 1965 *Phys. Rev.* **140** A1133
[21] Perdew J P, Burke K and Ernzerhof M 1996 *Phys. Rev. Lett.* **77** 3865
[22] Blöchl P E 1994 *Phys. Rev.* B **50** 17953
[23] Kresse G and Furthmüller J 1996 *Phys. Rev.* B **54** 11169
Kresse G and Furthmüller J 1996 *Comput. Mater. Sci.* **6** 15–50
[24] Kresse G and Joubert D 1999 *Phys. Rev.* B **59** 1758
[25] MedeA®-2.17 Materials Design, Inc., Angel Fire, NM, USA 2015
[26] Dudarev S, Botton G, Savrasov S, Humphreys C T and Sutton A 1998 *Phys. Rev.* B **57** 1505
[27] Piyanzina I I, Lysogosrkiy Yu V, Varlamova I I, Kiiamov A G, Kopp T, Eyert V, Nedopekin O V and Tayurskii D A 2016 *J. Low Temp. Phys.* **185** 597
[28] Zhong Z, Tóth A and Held K 2013 *Phys. Rev.* B **87** 161102
[29] Zabaleta J *et al* 2016 *Phys. Rev.* B **93** 235117
[30] Pentcheva R and Pickett W 2009 *Phys. Rev. Lett.* **102** 107602
[31] Schwingenschlögl U and Schuster C 2009 *Chem. Phys. Lett.* **467** 354